11. J. G. Meitín and J. B. Cunning, *NOAA Tech. Memo ERL ESG-20* (National Oceanic and Atmospheric Administration, Boulder, CO, 1985).
12. R. A. Houze, *Mon. Weather Rev.* **105**, 1540 (1977), E. J. Zipser, *ibid.*, p. 1568.
13. NASA, "Chemical kinetics and photochemical data for use in stratospheric modeling" (Publ. 85-37, Jet Propulsion Laboratory, Pasadena, CA, 1985).
14. We thank D. Apple, R. Brown, J. Cunning, S. Fink, B. Gockel, L. Gunter, D. Kita, P. Klotz, D. Leahy, J. Meitin, D. Rodenhuis, D. Wellman, and L. Wolpert who contributed to the success of the project. We also thank the Research Aviation Facility staff of NCAR, notably, R. Burris, E. Miller, and J. Ragni; . A. Schanot was especially helpful. Discussions with R. Chatfield, P. Crutzen, and E. Zipser were enlightening. This report was taken from a dissertation to be submitted to the Graduate School, University of Maryland, by W.T.L. in partial fulfillment of the requirements for the Ph.D. degree in chemistry. This work was conducted under the joint sponsorship of NSF (grant ATM-83-05843 and PRE-STORM), Department of Energy (PRECP), and NOAA (PRE-STORM). NCAR is sponsored by NSF.

14 July 1986; accepted 31 October 1986

Validity Tests of the Mixing-Length Theory of Deep Convection

KWING L. CHAN AND SABATINO SOFIA

The construction of solar or stellar models is hindered by the difficulty of computing, with sufficient accuracy, the convective fluxes in unstable regions. Although the mixing-length theory of convection has been used for more than three decades, its validity has neither been tested by experiment nor verified by computation. This report presents the results of a three-dimensional numerical simulation of deep and efficient convection that support two conclusions: (i) the basic picture proposed by the mixing-length theory is physically valid—the vertical correlation of the motion of fluid elements is proportional to the pressure scale height; and (ii) some dynamical variables, including the convective flux, can be approximately computed from the structure of the stratification with mixing-length approximations.

THE MIXING-LENGTH THEORY (MLT) of convection (*1, 2*) is at present the only practical approach for calculating convective fluxes in highly stratified convection zones. MLT is widely applied in many areas of astrophysical and geophysical fluid dynamics (*3, 4, 5*); in particular, a major part of solar and stellar theory depends on its validity. Despite this extensive use, the validity of MLT has remained controversial because it drastically simplifies the complex phenomenon of turbulent flow in a stratified compressible medium (*6*). Like any approximation, MLT will be inadequate to describe some features of the flow but possibly adequate for describing others. Thus, it would be useful to establish the domain of validity for the theory. Whereas many studies (for example, simulation of the solar granules or computation of the pulsation-convection coupling) require detailed dynamical information that cannot be provided by MLT, other studies, such as stellar evolution, depend primarily on global flux information. A likely area of success for MLT is therefore the flux computation. We report results of numerical simulations that support the validity of two key elements of MLT, namely, the mixing-length concept itself, and the determination of the local dynamical variables that are essential to the flux calculation.

The average heat (enthalpy) flux, F, carried by the convective motions in an efficiently convecting layer is given by

$$F = \rho C_p C(V_z,\Delta T)V'T' \qquad (1)$$

where ρ is the density, C_p is the specific heat for constant pressure, and $C(V_z,\Delta T)$ is the correlation between the vertical velocity V_z and the temperature fluctuation ΔT, whose root-mean-square values are V' and T', respectively. MLT assumes that the convective heat transfer is performed by "bubbles" associated with temperature fluctuations. After traveling a characteristic distance, the mixing length ℓ, the bubbles "dissolve" back into the environment, so that V' and T' can be determined as (*7*)

$$V' \simeq (gH\Delta\nabla)^{1/2}\,(\ell/H) \qquad (2)$$

$$T' \simeq T\Delta\nabla(\ell/H) \qquad (3)$$

where g is the gravitational acceleration, H is the pressure scale height,

$$\Delta\nabla = \frac{\partial \ln(T)}{\partial \ln(p)} - \left[\frac{\partial \ln(T)}{\partial \ln(p)}\right]_{ad} \qquad (4)$$

is the superadiabatic gradient, which is a measure of how far the stratification is away from static stability, and p is the pressure. Note that the symbol $\simeq$ in the above equations absorbs factors of order unity which would not alter the fundamental scaling relations. The choice of ℓ is a serious uncertainty of MLT. The usual assumption is that $\ell = \alpha H$, where α, the mixing-length ratio, is a constant of order unity; however, some investigators prefer to use the density scale height instead of H as the scale length (*8, 9*).

To assess the validity of the mixing-length theory and its assumptions, we solve the Navier Stokes equations for an ideal compressible gas to simulate deep and efficient convection. The domain of computation is a rectangular box having width 1.5 times the depth. The sides have periodic boundary conditions, and the top and bottom are impenetrable and stress-free. A constant energy flux is supplied at the bottom, and the value of entropy is fixed at the top. The initial distribution is polytropic (the temperature gradient is uniform, and the density is a power function of the temperature) and slightly superadiabatic. For the computation, we use units that make the density, pressure, and temperature at the top, and the total depth, all equal to 1. The initial state is perturbed by a weak velocity field in the form of a few regular cells. An implicit

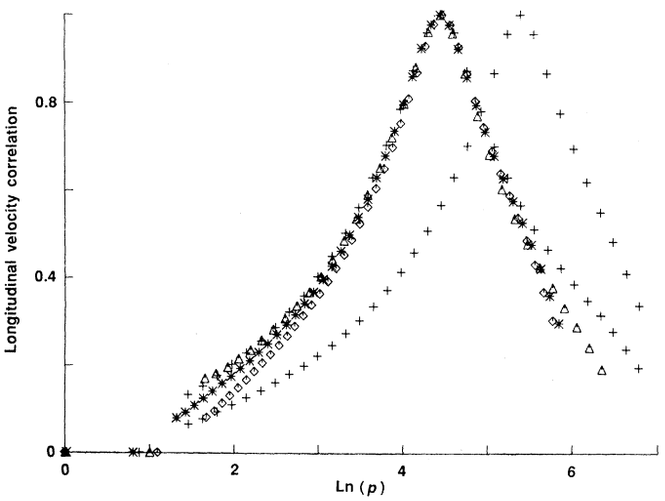

Fig. 1. Longitudinal correlation A of vertical velocities plotted against the logarithmic pressure $\ln p$ for the different numerical cases. (+) case a; (*) case b; (◇) case c; (△) case d, which has a different value of γ from the other three cases.

K. L. Chan, Applied Research Corporation, Landover, MD 20785.
S. Sofia, Center for Solar and Space Research, Yale University, New Haven, CT 06511.

numerical scheme (*10*) is used to compute the self-consistent, thermally relaxed structure of the convective layer (in a Kelvin-Helmholtz time); then a more accurate, second-order explicit numerical scheme is used to continue the computation for accumulating the flow statistics. The velocity field of the statistically stationary state is turbulent. A detailed description of our model and an examination of the validity and limitation of our numerical approach can be found elsewhere (*11*).

Four cases have been computed and their characteristics are summarized in Table 1. These cases have different ratios of specific heats, $\gamma = C_p/C_v$ which make the ratios of the scale heights different (since density scale height/pressure scale height = γ for an almost adiabatic atmosphere). The lower value of γ is representative of a hydrogen ionization zone, and the higher value is appropriate for fully ionized gases. The input fluxes are different so that the effects of different strengths of convection can be studied. The numerical grids are different so that invariance of results can be tested. The effective Reynolds number has values on the order of 300.

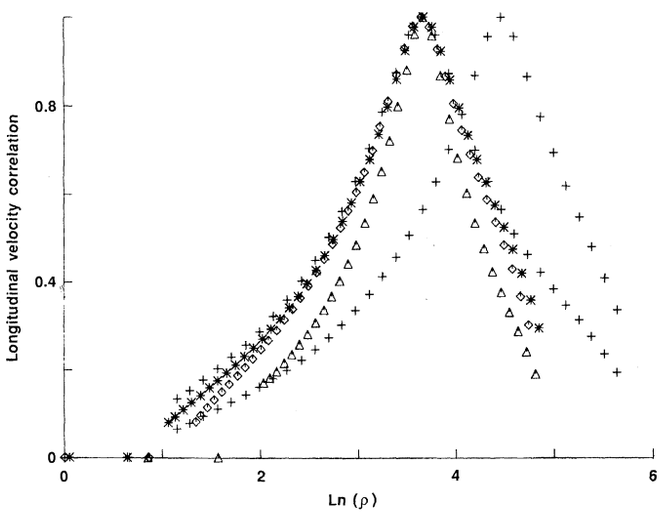

Fig. 2. Longitudinal correlation A plotted against the logarithmic density, ln ρ. For an explanation of the symbols, see the legend to Fig. 1.

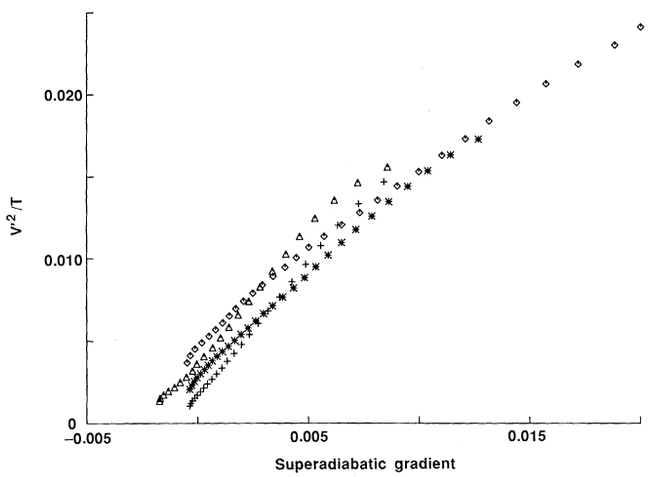

Fig. 3. The mean square vertical velocity V'^2 divided by the mean temperature T plotted against the mean superadiabatic gradient. For an explanation of the symbols, see legend to Fig. 1.

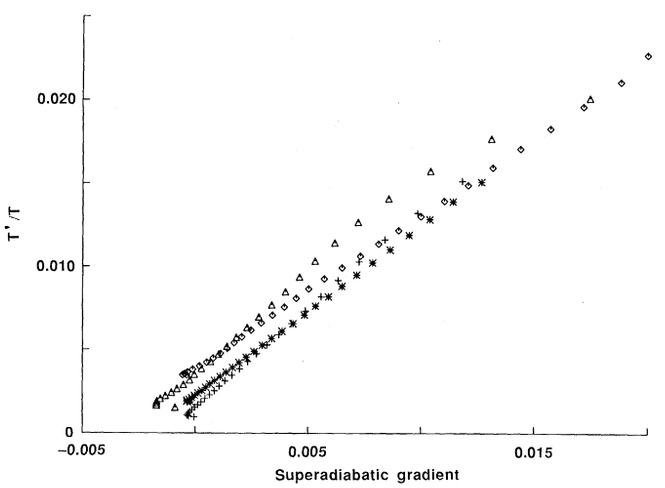

Fig. 4. The relative temperature fluctuation T'/T plotted versus the mean superadiabatic gradient. For an explanation of the symbols, see the legend to Fig. 1.

First, we look at the behavior of the longitudinal correlation function, A, for the vertical velocity of the turbulent flows:

$$A = \frac{\langle V_1 V_2 \rangle}{\langle V_1^2 \rangle^{1/2} \langle V_2^2 \rangle^{1/2}} \quad (5)$$

Here, V_1 and V_2 are the vertical velocities at two different vertical positions labeled by the subscripts 1 and 2. The brackets denote the combined average over time and horizontal position. The correlation length over which this function drops substantially (from 1 to 0.5, for example) characterizes the local size of the energy-containing eddies of the turbulence. In terms of the mixing-length interpretation, this length is also the vertical distance over which a convective bubble can preserve its identity. Figure 1 shows A versus the logarithmic pressure (ln p) for the different cases. For case a, two distributions for different depths are plotted; the similarity of these distributions illustrates that A is essentially a function of only the difference in the logarithmic pressures between the vertical positions 1 and 2; it is not dependent on the depth. The distributions for all the cases essentially coincide. In Fig. 2, the same distributions of A are plotted against the logarithmic density. The cases with different values of γ clearly show different widths. Therefore, the correlation length is scaled by the pressure scale height, not by the density scale height as some versions of MLT require. Furthermore, the agreement of cases b and c indicates that the correlation length does not depend on the magnitude of the convective flux. The agreement of cases a and b shows that this result does not depend on the numerical grids. The half-width at half maximum of A in Fig. 1 is approximately 1, which is compatible with α being of order unity.

Next, in terms of our units specified above, $gH = T$, and Eq. 2 can be rewritten as:

$$V'^2/T \simeq \alpha^2 \, \Delta\nabla \quad (6)$$

This expression is independent of γ and g, as long as the mixing length is a constant multiple of H. The mean square vertical velocity divided by the mean temperature versus the mean superadiabatic gradient for the numerical cases is plotted in Fig. 3. Only points for vertical positions far enough

Table 1. Characteristics of the computed cases.

Case	γ	Flux*	Grid†
a	20/17	0.125	20 × 20 × 37
b	20/17	0.125	20 × 20 × 46
c	20/17	0.333	20 × 20 × 46
d	5/3	0.125	20 × 20 × 37

*Dimensionless in the numerical simulation. †Number of mesh points: horizontal × horizontal × vertical.

($>H$) away from the top or bottom boundaries are plotted here to avoid contamination by boundary effects (at both ends, the vertical velocities are forced to vanish by the boundary conditions). All the points lie close to a straight line. However, the intercept of this line with the vertical axis is not zero; there is some residual velocity even when $\Delta\nabla$ approaches zero. The slope of the straight line is close to 1. Similarly, one would expect from Eq. 3 that T'/T varies linearly with $\Delta\nabla$ if α is constant. The temperature ratio is plotted versus the superadiabatic gradient in Fig. 4, which looks very similar to Fig. 3. The slope for these relations would also be close to 1. These results reinforce the validity of assuming that the mixing-length is proportional to the pressure scale height; they also demonstrate the feasibility of directly relating the mean dynamics to the mean atmospheric structure by simple relations similar to those given by the local MLT, in the limit that the convection is deep and efficient. Finally, the correlation, $C(V_z,\Delta T)$ is constant and has a value of about 0.8. Therefore, with Eq. 1, one can calculate the flux from a knowledge of $\Delta\nabla$, or vice versa.

The above results indicate that some basic assumptions made in computing coarse features of convection by means of MLT are valid, at least in the limited parameter range in which our numerical simulations were performed. However, one should not consider our results as a blanket confirmation of MLT. First, the parameter range of our computation does not cover all possible situations; for example, the values of the superadiabatic gradient are much smaller than those expected in the convective-radiative transition-layers where convection becomes less efficient but MLT is needed most. Second, much detailed dynamical information obtained by our simulation cannot be predicted by MLT. Consequently, problems that are sensitive to these details are not properly addressed by the MLT approach.

REFERENCES AND NOTES

1. L. Biermann, *Z. Astrophys.* **5**, 117 (1932).
2. E. Vitense, *ibid.* **32**, 135 (1953).
3. I. Iben, in *Stellar Evolution*, H. Y. Chiu and A. Muriel, Eds. (MIT Press, Cambridge, 1972), pp. 1–106.
4. F. Meyer and E. Meyer-Hofmeister, *Astron. Astrophys.* **106**, 34 (1982).
5. P. H. Stone, in *Jupiter*, T. Gehrels, Ed. (Univ. of Arizona Press, Tucson, 1976), pp. 587–618.
6. D. Gough and E. A. Spiegel, in *Problems of Stellar Convection*, E. A. Spiegel and J. P. Zahn, Eds. (Springer-Verlag, New York, 1977), pp. 57–62.
7. J. P. Cox and R. T. Giuli, *Principles of Stellar Structure* (Gordon and Breach, New York, 1968), pp. 281–325.
8. E. J. Opik, *Publ. Astron. Obs. Univ. Tartu* **301**, No. 3, (1938).
9. M. Schwarzschild, *Astrophys. J.* **134**, 1 (1961).
10. K. L. Chan and C. L. Wolff, *J. Comput. Phys.* **47**, 109 (1982).
11. K. L. Chan and S. Sofia, *Astrophys. J.* **307**, 222 (1986).

12. This research was partially supported by the National Science Foundation (grant AST-8504399). K.L.C. expresses his gratitude to P. Pesch for his encouragement.

28 August 1986; accepted 8 December 1986

The Glucocorticoid Receptor Protein Binds to Transfer RNA

MASARRAT ALI AND WAYNE V. VEDECKIS

The glucocorticoid receptor from mouse AtT-20 cells exists in three forms: (i) the untransformed receptor (9.1*S*; M_r of 319,000), a large oligomeric molecule that does not bind to DNA; (ii) the transformed receptor (4*S*; M_r of 96,000), which is formed by dissociation of untransformed receptor after steroid binding and which binds to DNA to modulate gene expression; and (iii) an intermediate size receptor (6*S*; M_r of 132,000), which also binds to DNA and contains a bound small RNA molecule. This RNA species has now been purified and identified as transfer RNA (tRNA). The three tRNA's for the basic amino acids accounted for about 78% of the total amino acid–accepting activity [arginine (52%), lysine (17%), and histidine (9%)], while the remaining 22% was represented by six other tRNA species. This tRNA-binding activity of the glucocorticoid receptor may reflect post-transcriptional mechanisms of regulating gene expression, such as alterations in the translational efficiency of or the modulation of the stability of hormone-induced proteins.

ALTHOUGH THE UNTRANSFORMED glucocorticoid receptor (GR) from mouse AtT-20 cells (*1–5*) contains no detectable bound RNA (*6*), RNA-binding activity has been demonstrated for the transformed estrogen (*7–9*), progesterone (*7*), androgen (*7, 10*), vitamin D (*10, 11*), and glucocorticoid (*4–7, 12–14*) receptor proteins [reviewed in (*3*)]. Thus, it appears that dissociation of subunits from the untransformed complex leads to the formation of the monomeric 4*S* GR (*2*) and the monomeric GR subsequently binds to small RNA molecules in the cytosolic extract, leading to formation of the 6*S* RNA–containing GR form. We have previously been able to reconstitute the 6*S* GR from partially purified 4*S* GR monomer and RNA (*4*). We therefore used the conversion of the 4*S* GR monomer to the 6*S* form by the addition of exogenous RNA as an assay for purification of this RNA.

RNA capable of shifting the 4*S* monomeric GR to 6*S* on sucrose gradients was purified by DEAE-cellulose chromatography, hydroxylapatite chromatography, sucrose gradient ultracentrifugation, and selection for RNA that was not polyadenylated on oligo dT–cellulose. The purified RNA [PIVB RNA: pool IV from DEAE-cellulose (eluted at 0.35*M* to 0.45*M* KCl), B (4*S*) pool from preparative sucrose gradients; see Fig. 1] was indistinguishable in size from yeast transfer RNA (tRNA) (mixture of several tRNA's) or purified *Escherichia coli* tRNA specific for valine or glutamic acid when analyzed on ethidium bromide–stained agarose gels. PIVB RNA was also indistinguishable from tRNA in its sedimentation coefficient (4*S*) on sucrose gradients. We treated the purified PIVB RNA preparation with calf intestinal alkaline phosphatase and then labeled it at the 5′ end with ^{32}P using polynucleotide kinase. We obtained three predominant ^{32}P-labeled bands—74 (minor), 76 (major), and 78 (minor) nucleotides (Fig. 1). Detectable amounts of ^{32}P-labeled RNA that were both larger and smaller than these species were also present. The fact that we could label the PIVB RNA demonstrated that it was not capped and, therefore, was not an RNA polymerase II transcript.

Several characteristics of PIVB RNA suggested that it contained tRNA: its size (76 nucleotides), the 4*S* sedimentation coefficient, the large amount obtained from the

Department of Biochemistry and Molecular Biology, Louisiana State University Medical Center, New Orleans, LA 70112.